0013-7227/06/$15.00/0
Printed in U.S.A.

Endocrinology 147(8):3915–3923

doi: 10.1210/en.2006-0277

Congenic Mice Provide *in Vivo* Evidence for a Genetic Locus that Modulates Serum Insulin-Like Growth Factor-I and Bone Acquisition

K. M. Delahunty, K. L. Shultz, G. A. Gronowicz, B. Koczon-Jaremko, M. L. Adamo, L. G. Horton, J. Lorenzo, L. R. Donahue, C. Ackert-Bicknell, B. E. Kream, W. G. Beamer, and C. J. Rosen

The Jackson Laboratory (K.M.D., K.L.S., L.G.H., L.R.D., C.A.-B., W.G.B., C.J.R.), Bar Harbor, Maine 04609; The University of Connecticut Medical Center (G.A.G., B.K.-J., J.L., B.E.K.), Farmington, Connecticut 06030; and The University of Texas Health Sciences Center at San Antonio (M.L.A.), San Antonio, Texas 78229

We identified quantitative trait loci (QTL) that determined the genetic variance in serum IGF-I through genome-wide scanning of mice derived from C57BL/6J(B6) × C3H/HeJ(C3H) intercrosses. One QTL (*Igf1s2*), on mouse chromosome 10 (Chr10), produces a 15% increase in serum IGF-I in B6C3 F2 mice carrying *c3* alleles at that position. We constructed a congenic mouse, B6.C3H-10 (10T), by backcrossing *c3* alleles from this 57-Mb region into B6 for 10 generations. 10T mice have higher serum and skeletal IGF-I, greater trabecular bone volume fraction, more trabeculae, and a higher number of osteoclasts at 16 wk, compared with B6 ($P < 0.05$). Nested congenic sublines generated from further backcrossing of 10T allowed for recombination and produced four smaller sublines with significantly increased serum IGF-I at 16 wk (*i.e.* 10-4, 10-7, 10-10, and 10-13), compared with B6 ($P < 0.0003$), and three smaller sublines that showed no differences in IGF-I *vs.* age- and gender-matched B6 mice. Like 10T, the 10-4 nested sublines at 16 wk had higher femoral mineral ($P < 0.0001$) and greater trabecular connectivity density with significantly more trabeculae than B6 ($P < 0.01$). Thus, by comprehensive phenotyping, we were able to narrow the QTL to an 18.3-Mb region containing approximately 148 genes, including *Igf1* and *Elk-3*(ETS domain protein). Allelic differences in the *Igf1s2* QTL produce a phenotype characterized by increased serum IGF-I and greater peak bone density. Congenic mice establish proof of concept of shared genetic determinants for both circulating IGF-I and bone acquisition. (*Endocrinology* 147: 3915–3923, 2006)

CIRCULATING IGF-I IS A COMPLEX trait with multiple genetic and environmental determinants (1). Studies in mice, baboons, rats, and humans have also demonstrated strong heritability for bone mineral density (BMD) and peak skeletal acquisition, although identifying those genes has not been straightforward (2–4). *Igf1* is an attractive candidate gene for bone acquisition because it is a circulating and skeletal mediator of GH action (5). Targeted genomic studies have confirmed the importance of skeletal IGF-I for the osteoblast differentiation program and osteoclastogenesis (6–8). Similarly, circulating IGF-I affects bone modeling and appears to cosegregate with BMD in several mouse models (1, 5, 9–11). Support for the premise that genetic regulation of circulating IGF-I may play an important role in peak bone acquisition comes from both human and mouse studies. In the former, several polymorphisms in the P1 promoter and the 3′-untranslated region of the *Igf1* gene have been associated with BMD, skeletal geometry, and serum IGF-I (9, 10). In respect to the latter, studies with inbred strains of mice have demonstrated strong heritability for the serum IGF-I phenotype and a close correlation with volumetric femoral BMD (vBMD) (11, 12). Recently we reported that differences in serum IGF-I between two inbred strains of mice were due to increased P2 promoter activity of the *Igf1* gene, thereby suggesting that heritability of this phenotype was related to one or more genetic determinants functioning either as *cis* or *trans* acting factors to regulate gene transcription (13, 14).

To overcome the difficulty in finding genes that influence IGF-I, we turned to a quantitative trait locus (QTL) approach using two inbred strains of mice. As reported previously, C3H/HeJ (C3H) female mice have greater serum IGF-I concentrations as well as higher vBMD than C57BL/6J (B6) during and after development (2, 11, 12, 15). By crossing C3H and B6 and then intercrossing B6C3F1 mice, we identified several QTL in the female F2 progeny that independently segregated for serum IGF-I and femoral BMD (2, 12). Three QTL for IGF-I were found to contribute about 50% of the variance across the two strains and two of these (*i.e. Igf1s1, Igf1s2*) could be superimposed on femoral BMD QTL (2, 12). Previously we reported genomic and functional studies for one congenic strain, B6.C3H-6T (*i.e.* 6T, which carries the *Igf1s1* QTL) (16–19). In this study, we examined the IGF-I and skeletal phenotypes of a second congenic mouse strain, B6.C3H-10 (*i.e.*10T). This strain carries the *Igf1s2* QTL on a B6 background with C3H alleles from the midportion of chromosome (Chr) 10. Based on previous F2 data for both the serum IGF-I phenotype and vertebral trabecular bone volume fraction (BV/TV), we predicted, *a priori*, that a congenic

First Published Online May 4, 2006

Abbreviations: BMC, Bone mineral content; BMD, bone mineral density; BV/TV, trabecular bone volume fraction; Chr, chromosome; DXA, dual-energy x-ray absorptiometry; IGFBP, IGF binding protein; microCT, micro-computed tomography; pQCT, peripheral quantitative computed tomography; QTL, quantitative trait loci; RPA, RNase protection assay; SMI, structure model index; vBMD, volumetric femoral BMD.

***Endocrinology* is published monthly by The Endocrine Society (http://www.endo-society.org), the foremost professional society serving the endocrine community.**

strain with this 30-cM region of the Chr 10 genome from C3H would show increased serum IGF-I and greater bone mass (12, 15). Findings from several nested congenic sublines indicated that allelic differences in this QTL profoundly affect both circulating IGF-I and skeletal remodeling.

Materials and Methods

Mice

The progenitor inbred strains, C3H/HeJ(C3H) and C57BL/6J(B6), are available from The Jackson Laboratory (Bar Harbor, ME; C3H (Jax Research no. 000659) and B6 (Jax Research no. 000664). BMD and IGF-I data on these two strains have been published previously (2, 11, 15). The congenic strain, B6.C3H-10T (10T), was generated by introgressing a region of Chr 10 from C3H into a B6 background for 10 generations. This region contains *Igfsl2*, a QTL affecting serum IGF-I (12). Recombination of 10T mice through intercrossing brother-sister pairs led to the generation of 10T sublines, numbered by their production. Currently there are eight sublines (10-1, 10-2, 10-3, 10-4, 10-5, 10-7, 10-10, 10-13) that have been fully genotyped and phenotyped for serum IGF-I at 8 and 16 wk of age. There are two congenic sublines with complete skeletal phenotyping: 10T and 10-4. Bone parameters in the sublines reported in this study, *i.e.* 10T and 10-4, are always compared with age- and gender-matched B6 progenitors. The animal protocol was approved by Institutional Animal Care and Use Committee at The Jackson Laboratory.

Phenotyping

Dual-energy x-ray absorptiometry (DXA) scanning by PIXImus. We used PIXImus (GE-Lunar, Madison, WI) to assess areal whole-body BMD and body composition in 10T congenic and B6 control mice at 8 and 16 wk of age. This methodology has been validated in small animals. PIXImus scanning in mice for bone mineral content (BMC) and percent fat is both accurate and precise, although size must be considered when comparing strains. BMC by PIXImus is highly correlated with mineral content of hydroxyapatite standard of known density ($r^2 = 0.997$).

Peripheral quantitative computed tomography (pQCT) for volumetric femoral BMD. vBMD was measured on the entire left femur from groups of female and male B6 and congenic mice. Isolated femur length was measured with digital calipers (Stoelting, Wood Dale, IL), and then femurs were measured for density using the SA Plus densitometer (Orthometrics; Stratec SA Plus Research Unit, White Plains, NY). Calibration of the SA Plus instrument was done with hydroxyapatite standards of known density (50–1000 mg/mm^3) with cylindrical diameters 2.4 mm and length 24 mm. Assessment of defined thickness aluminum foils indicated accurate measurement of the 0.25-mm-thick foil, whereas a 0.02-mm-thick foil could not be measured. The bone scans were analyzed with two different sets of thresholds to separate bone from soft tissue. Outer high density thresholds of 710 and 570 mg/cm^3 were used to determine cortical bone areas and surfaces. This threshold was selected to yield area values consistent with histomorphometrically derived values. To determine mineral content, a second analysis was carried out with threshold settings of 220 and 400 mg/cm^3. These lower thresholds were selected so that mineral from most partial voxels (0.07 mm) would be included in the analysis. Density values were calculated from the summed areas and associated mineral contents. Precision of the SA Plus for repeated measurement of a single femur was found to be 1.2%. Isolated femurs were scanned at seven locations at 2-mm intervals, beginning 0.8 mm from the distal ends of the epiphyseal condyles. Due to variation in femur lengths, the femoral head and necks could not be scanned at the same location for each bone and thus was not included in final data. Total vBMD values were calculated by dividing the total mineral content by the total bone volume (bone + marrow) and expressed as milligrams per cubic millimeter. Periosteal perimeters and cortical thickness data were obtained at the midshaft scan.

MicroCT (micro-computed tomography) 40 femoral cross-sectional geometry and trabecular morphology. Femurs from age-, genotype-, and gender-matched mice were scanned using a microCT40 microcomputed tomographic instrument (μCT40, Scanco Medical AG, Bassersdorf, Switzerland) to evaluate cross-sectional geometry at the femoral midshaft and trabecular bone volume fraction and microarchitecture in the secondary spongiosa of the distal femur (15). The femurs were scanned at low resolution, energy level of 55 KeV, and intensity of 145 μA. Eighteen slices were measured at the midpoint of each femur, with an isotropic pixel size of 12 μm and slice thickness of 12 μm, and used to compute the average total cross-sectional area (square millimeters), bone area (square millimeters), marrow area (square millimeters), and cortical thickness (micrometers). Images of the distal femur were acquired at the same parameters as the femoral midshaft. BV/TV and microarchitecture were evaluated in the secondary spongiosa, starting at approximately 0.6 mm proximal to the growth plate and extending proximally 1.5 mm.

IGF-I measurements

Serum IGF-I was measured by a RIA (ALPCO, Windham, NH) (16). IGF binding proteins (IGFBPs) were first separated from the IGF-I by an acid dissociation step. This was followed by the addition of a neutralization buffer containing excess recombinant human IGF-II, allowing the IGF-II to bind to the IGFBPs before immunoassay with a human anti-IGF-I polyclonal antibody. The sensitivity of the assay is 0.01 ng/ml IGF-I; the interassay coefficient of variation based on normal standards and pooled serum of C3H and B6 is approximately 6%. There is no cross-reactivity with IGF-II. Standards were included in each assay as well as normal pools from both progenitors. Because of the large numbers of samples run for IGF-I, all values were adjusted to the standard B6 mouse pools using a correction factor to account for interassay variation. In addition to serum measurements, IGF-I in conditioned media was measured using the same assay; the results were then corrected for milligrams of protein in the conditioned medium (*i.e.* nanograms per milligram of protein).

Quantitative PCR

Samples of liver and bone tissue from 8-wk 10T and B6 controls male mice were extracted for RNA as previously described (17). Briefly, total RNA was isolated from liver and bone using the Total RNA isolation system (Promega, Madison, WI) as per the manufacturer's instructions. RNA was DNAase treated and subsequently purified further using RNA Easy spin columns (QIAGEN, Valencia, CA). RNA quality and quantity were assessed using an Agilent bioanalyzer (Caliper Technologies Corp., Hopkinton, MA). Five hundred nanograms of RNA was converted to cDNA in a reverse transcription reaction, using Superscript II (no. 18064-014; Invitrogen, Carlsbad, CA) and random hexamers as primers as per the manufacturer's direction. The cDNA was then diluted 1:5 with water. For each PCR, 1 μl of diluted cDNA was added to 5 μl of 2 $\times$ iTaq SYBR Green Supermix with ROX (catalog no. 170-8851; Bio-Rad Laboratories, Hercules, CA) and 100 nM of each forward and reverse primer in a total reaction volume of 10 μl. Cycling conditions were 2 min hold at 50 C; 3 min hold at 95 C; 40 cycles of 95 C, 15 sec; 60 C, 1 min; and all reactions were run on the ABI 7900HT sequence detection system (Applied Biosystems, Warrington UK). Each of the 48 sets of gene-specific primers was analyzed by real-time PCR to assess transcript levels, with each primer pair run once per biological replicate. Four biological replicates were run per strain. Differential expression was assessed using a global pattern recognition algorithm (GPR) as previously described (20). In short, the global pattern recognition algorithm assesses each gene as a potential normalizer for all other genes on the run. It then calculates a score based on the fraction of normalizers against which a given gene was found to be significantly different. Fold change is then calculated as previously described (20, 21). In this manner the statistical significance of an observed expression level difference is assessed before fold change is calculated. With numerous normalizers used per examined gene, biases based on any one normalizer are eliminated.

IGF-I RNase protection assay

A 386-bp DNA fragment consisting of the 3′ end of intron 1, the entire 72 bp of exon 2, the contiguous 241 bp containing exon 3, and the 5′ end of exon 4 was obtained from a mouse IGF-I clone and was subcloned into pGEM 2 (13). The plasmid was linearized with *Eco*R1, and T7 RNA polymerase was used to synthesize a ^{32}P-labled antisense RNA using α-^{32}P-UTP (DuPont NEN Life Science Products, Boston, MA) and re-

agents from Ambion, Inc. (Austin, TX). The probe was hybridized with equivalent amounts of total RNA. Hybridization, subsequent RNase digestion of unhybridized RNA and collection, and electrophoresis of protected probe fragments were carried out as described by Adamo *et al.* (13). Hybridization of the probe to IGF-I mRNAs yields a protected band of 241 nt, reflecting exon 1 transcripts, and a series of bands ranging from approximately 290 to approximately 310 bp, reflecting IGF-I mRNAs initiated from the clusters of exon 2 start sites. RNase protection assays (RPA) for mouse actin used a construct, also supplied by Ambion.

Histomorphometry

Femurs were dissected free of tissue and fixed in 4% paraformaldehyde at the time the animals were killed. The undecalcified femurs were then dehydrated in increasing concentrations of ethanol, cleared in xylene, and embedded in methyl methacrylate. Five-micrometer-thick longitudinal serial sections were cut on a Reichert-Jung Polycut S microtome (Reichert-Jung, Heidelberg, Germany). Sections were taken from the middle of the femur, in which a central vein is located. Some sections were stained with modified Masson trichrome stain for static measurements (22). Histomorphometric measurements were made in a blinded, nonbiased manner using the OsteoMeasure computerized image analysis system (OsteoMetrics, Inc., Atlanta, GA) interfaced with an Optiphot Nikon microscope (Nikon Inc., Melville, NY) at a magnification of ×20. The terminology and units used are those recommended by the Histomorphometry Nomenclature Committee of the American Society for Bone and Mineral Research (23). All measurements were confined to the secondary spongiosa and restricted to an area between 400 and 2000 m distal to the growth plate-metaphyseal junction of the distal femur. Cortical measurements were made 4000 m distal to the same growth plate.

Adult bone marrow stromal cell cultures for IGF-I

Bone marrow was removed from 10T and B6 8-wk-male mice and immediately plated in dishes. Adherent cells were removed after 2 d, and these cells were plated in six-well dish plates and cultured for 7 d in DMEM and 10% fetal calf serum with medium change at d 3. After 7 d, medium was replaced with αMEM, glycerophosphate, and phosphoascorbate. After 24 h, the conditioned medium is removed and assayed for both IGF-I and protein content.

Statistics

Data are expressed as mean ± SEM in tables and figures. Statistical evaluation was performed using the JMP (SAS, Cary, NC) ANOVA software program for ANOVA and for linear model regression analyses. The pQCT data were adjusted for effects of body weight and femur length, whereas the DXA (PIXImus) data were adjusted for effects of body weight. Differences between adjusted least squares means for B6 and each congenic subline were tested by Student's *t* test, with significance declared when $P < 0.05$ was observed. Differences between 8 and 16 wk in serum IGF-I for B6 and the congenic sublines were also tested by ANOVA.

Results

10T congenic mice: circulating, skeletal, and hepatic expression of IGF-I

Congenic 10T mice (N10F2) were generated by introgressing the locus on Chr 10 (*i.e. Igf1s2*) into a B6 background for 10 generations; details of this technique have previously been reported by our group and others (15). Congenic 10T mice have a background that is 99.6% B6 but carry C3H (*c3*) alleles at one locus (*i.e.* midregion of Chr 10); they do not differ from B6 with respect to birth weight, reproductive capacity, or food consumption. At 8 wk, there was a trend for male 10T mice to have slightly but not significantly greater levels of IGF-I than B6 ($P = 0.20$); female 10Ts at 8 wk did not differ from B6 ($P = 0.90$). But at 16 weeks, we noted higher serum IGF-I concentrations in both male and female 10T mice, compared with age-matched B6 (n = 15 mice per genotype per gender; male 10T: 280 ± 8 *vs.* B6: 233 ± 7 ng/ml; $P = 0.0002$; female 10T: 287 ± 10 *vs.* B6: 265 ± 7 ng/ml $P = 0.09$). At 20 wk of age, 10T mice of both genders (n = 15 per gender) showed significant differences from B6: male 10T: 330 ± 5.9 *vs.* B6: 304 ± 5.6 ng/ml; $P = 0.002$; female 10T: 341 ± 8.8 *vs.* B6: 317 ± 6.9 ng/ml, $P = 0.03$. Despite these IGF-I strain differences, no consistent changes in circulating IGFBPs for 10T, compared with B6, were noted at 16 wk as measured by Western ligand blot (data not shown).

The differences in serum IGF-I were mirrored by expression changes in the liver as determined by RPAs. Eight-week 10T male mice (n = 6 per strain) showed significantly increased exon 2 transcripts of the *Igf1* gene, compared with B6 (n = 4) ($P < 0.05$) (Fig. 1), a pattern identical with what has been reported for progenitor C3H hepatic transcripts of *Igf1* (13). RT-PCR of 8-wk male liver from 10T and B6 confirmed a 1.8 ± 0.6-fold greater expression of *Igf1* mRNA in 10T *vs.* B6 ($P < 0.05$). Similarly, in three determinations of 8-wk whole femorae (*i.e.* cortical and trabecular bone plus marrow contents), skeletal *Igf1* mRNA by RT-PCR was 1.33 ± 0.08-fold greater in 10T than B6 ($P < 0.05$). Expression differences in IGF-I in whole bone were also reflected by strain differences in secreted IGF-I from conditioned media of adult bone marrow stromal cells (*i.e.* 10T IGF-I secreted: 579 ± 41 ng/mg protein *vs.* B6 IGF-I secreted: 350 ± 20 ng/mg protein, $P < 0.01$). Finally, two important skeletal factors also showed differential strain expression by quantitative PCR of long bones. In 10T mice, Runx2, a bone-specific transcription factor necessary for osteoblast differentiation, exhibited 1.63-fold greater mRNA expression relative to B6 ($P < 0.05$), whereas message for IGFBP-5, an IGFBP regulated by IGF-I, was 2.12-fold higher in 10T than B6 femorae ($P < 0.05$). Thus, serum IGF-I as well as hepatic and skeletal expression of IGF-I was greater in 10T than B6, a pattern also seen in C3H mice (13). Moreover, these strain differences were reflected in secreted IGF-I from adult marrow cells and the expression in bone of two downstream targets of IGF-1 activity, IGFBP-5 and Runx2.

Body composition and skeletal phenotyping of 10T

To determine how allelic changes in circulating and skeletal IGF-I affected body composition, we performed DXA scans by PIXImus in 16-wk 10T and B6 male and female mice. Female 10T mice had modestly higher lean body mass ($P < 0.08$ *vs.* B6) and slightly greater percent BMC, compared with B6, even though total body weight did not differ (Table 1). Volumetric BMD of the total femur and midshaft was measured by pQCT. 10T females had nearly identical femoral size as B6 females, with slightly but not significantly greater cortical thickness; there were no differences in cortical bone density or periosteal circumference between strains. Male 10Ts were not different from male B6 for any cortical parameter (data not shown).

When distal femoral BV/TV was measured by microCT, the strain differences between 10T and B6 were gender dependent. Female 10T had significantly higher trabecular BV/TV and trabecular number at 16 wk, compared with B6

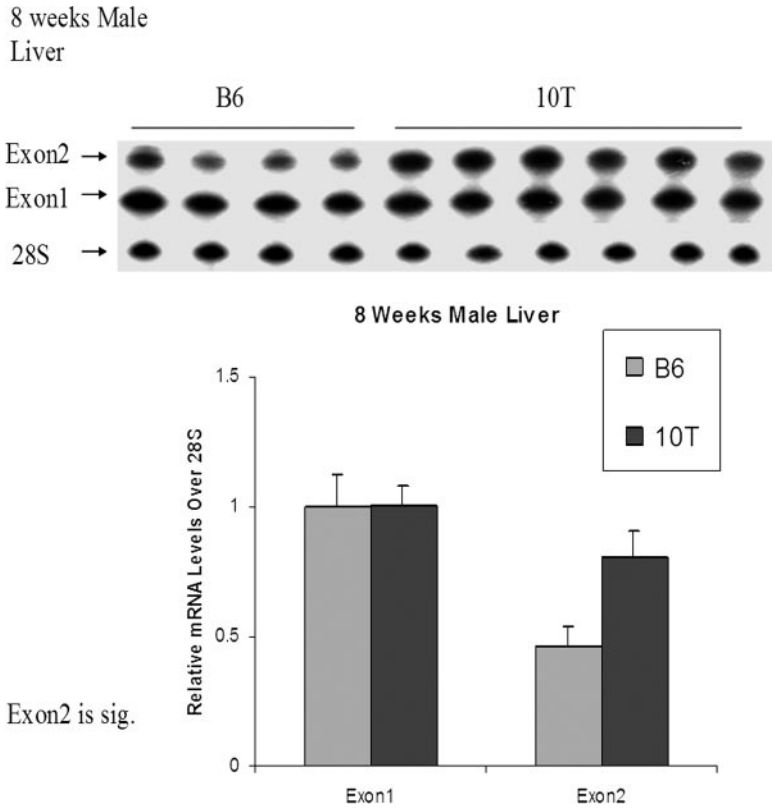

FIG. 1. RPA of IGF-I from B6 (n = 4) and 10T (n = 6) liver. Mean values for exon 2 but not exon 1 were different between B6 and 10T ($P < 0.05$).

($P < 0.01$; see Table 2). For male 10T mice, BV/TV was slightly but not significantly higher *vs.* B6, but like female 10T, trabecular number was markedly increased ($P < 0.005$) and there was a trend toward lower structure model index (SMI) (Table 2). We next performed dynamic bone histomorphometry from the distal femur of 16-wk congenic and B6 males and females (n = 11/strain). Once again, we found that female 10T mice had higher distal femoral BV/TV than B6 ($P < 0.05$). Also, the number of osteoclasts per bone perimeter and per bone surface was markedly increased in 10T females, compared with B6 females ($P < 0.01$). On the other hand, for males, there were strain differences, compared with B6, that paralleled female 10T changes, but these were not statistically significant (see Table 3).

Generation of nested congenic sublines for mapping and phenotyping

Because the *Igf1s2* QTL mapped by F2 analysis spanned more than 57 Mb of the C3H genome and was carried in the 10T strain, we estimated that more than 500 genes could be contributing to the phenotypic differences between 10T and B6. Hence, to narrow the genomic region and reduce the number of potential candidate genes, we generated nested sublines by backcrossing 10T to B6 and then fixing the recombinants (Fig. 2). We chose to study female nested congenics for two reasons: 1) we mapped the *Igf1s2* QTL in females only (12); and 2) differences in trabecular bone mass by microCT and histomorphometry were greatest in females. Fixed nested congenics as determined by comprehensive genotyping in the Chr 10 locus (see Fig. 2), were then tested for serum IGF-I at both 8 and 16 wk using a minimum of 10 mice per subline per age. We found that serum IGF-I at 8 wk was significantly greater in female 10-4, 10-7, 10-10, and 10-13 than B6 ($P < 0.05$ by ANOVA), and at 16 wk, sublines 10-4, 10-7, 10-10, and 10-13 were markedly greater than B6 (*i.e.* > 20% higher; $P < 0.0003$ by ANOVA; Fig. 3).

In the 10-4, 10-7, 10-10, and 10-13 nested sublines, serum IGF-I either increased or stayed the same between 8 and 16 wk of age, a finding similar to C3H progenitors measured during that same growth period (11). On the other hand, serum IGF-I in the B6 females consistently declined by at least 10% between 8 and 16 wk ($P = 0.03$ for serum IGF-I in B6 between 8 and 16 wk). Thus, the nested congenic sublines provided further proof of a small locus in the midregion of

TABLE 1. Body composition in 10T and B6 males and females at 16 wk of age

Strain/gender	n	Total tissue (g)	Lean tissue (g)	Lean (%)	BMC (%)
B6 males	14	26.82 ± 0.69	20.65 ± 0.30	77.7 ± 2.3	1.61 ± 0.60
10T males	15	25.21 ± 0.66	20.14 ± 0.29	79.0 ± 1.3	1.56 ± 0.60
B6 females	11	19.60 ± 0.66	15.74 ± 0.10	82.3 ± 1.1	1.97 ± 0.70
10T females	11	18.26 ± 0.71	15.91 ± 0.10	84.6 ± 0.6[a]	2.04 ± 0.70

Percent lean, BMC, and % fat corrected for total tissue value.
[a] $P < 0.08$, 10T females *vs.* B6.

TABLE 2. MicroCT parameters in distal femurs of 8- and 16-wk 10T and B6 male and female mice

Phenotype	B6 males	10T males	B6 females	10T females
8 wk	n = 16	n = 18	n = 18	n = 19
Total volume	2.416 ± 0.048	2.294 ± 0.043	2.008 ± 0.024	1.918 ± 0.022[a]
BV/TV	0.234 ± 0.012	0.235 ± 0.011	0.1186 ± 0.004	0.1255 ± 0.004
SMI	1.676 ± 0.089	1.701 ± 0.080	2.614 ± 0.038	2.563 ± 0.037
Trabecular thickness	0.053 ± 0.002	0.052 ± 0.001	0.0433 ± 0.0005	0.0419 ± 0.0004[a]
Trabecular no.	6.283 ± 0.079	6.684 ± 0.076[b]	5.089 ± 0.046	5.388 ± 0.045[b]
16 wk	n = 23	n = 20	n = 24	n = 22
Total volume	2.448 ± 0.037	2.549 ± 0.044	1.968 ± 0.020	2.090 ± 0.021
BV/TV	0.1950 ± 0.008	0.2033 ± 0.009	0.082 ± 0.003	0.096 ± 0.003[b]
SMI	1.794 ± 0.078	1.756 ± 0.093	2.969 ± 0.047	2.788 ± 0.050[b]
Trabecular thickness	0.053 ± 0.001	0.050 ± 0.001[a]	0.048 ± 0.001	0.049 ± 0.001
Trabecular no.	5.293 ± 0.053	5.641 ± 0.057[b]	3.788 ± 0.040	3.978 ± 0.043[b]

[a] $P < 0.05$ *vs.* B6.
[b] $P < 0.005$ *vs.* B6.

Chr 10 containing one or more genes that affected circulating IGF-I and was temporally regulated.

Skeletal phenotyping of the 10-4 subline

To determine whether the skeletal phenotype was carried in the first set of nested sublines with the highest IGF-I levels, we measured femoral vBMD and BV/TV at 16 wk in sublines with a minimum of 10 mice/strain; *i.e.*:10-1, 10-2, 10-3, 10-4, and B6 controls. Only subline 10-4 showed statistically significant differences in measurements of trabecular bone by microCT and cortical bone by pQCT from B6. Distal femoral bone volume, total femoral mineral, midcortical density, trabecular number, connectivity density, and SMI were all significantly different in 10-4, compared with B6 ($P < 0.02$ *vs.* B6 for all parameters, see Table 4). Other nested sublines showed no differences in trabecular or cortical parameters when compared with B6 (data not shown). Hence, greater circulating IGF-I in at least one nested subline was associated with enhanced bone mineral and mass.

Candidate genes in the Chr 10 QTL

The Chr 10 QTL is approximately 57 Mb in size, whereas the 10-4 region is less than 33 Mb. The latter region contains approximately 300 known genes and expressed sequence tags. However, with subline phenotyping for serum IGF-I, we were able to narrow the region to approximately 18.3 Mb and 148 genes (see Supplemental Fig. 1, published on The Endocrine Society's Journals Online web site at http://endo.endojournals.org). As shown in Fig. 2, 10-7, 10-10, and 10-13 have higher serum IGF-I than B6 at both 8 and 16 wk, whereas 10-1, 10-2, and 10-5 do not. The most obvious candidate gene carried within the sublines that show higher serum IGF-I is *Igf1* itself (Fig. 4). However, three other genes are of interest: *Socs2*, which is an inhibitor of growth hormone signaling; *Elk-3 (Ets* domain protein), which is an activator of transcription in the IGF-I signaling pathway; and *Kitl* (Kit ligand), which can stimulate osteoclastogenesis. Finally, it is worth noting that QTL for two other phenotypes that may be regulated by IGF-I, vertebral BV/TV and whole-body growth, have also been mapped to this region (15, 24; and http://www.informatics.jax.org) (see Fig. 4). Thus, using sublines as mapping tools, we can narrow the list of candidate genes and subsequently determine by differential expression and sequence analysis the genetic determinants of IGF-I within this locus.

Discussion

In this study, using the congenic 10T strain and its nested sublines as models, we demonstrated that allelic determinants in a gene or genes from the mid region of Chr 10 profoundly affect serum IGF-I and bone acquisition. We built the 10T congenic by introgressing about 57 Mb of the C3H genome on Chr 10 onto a B6 background. Two major phenotypes were considered a priori, IGF-I and BV/TV; these predictions were based on our previous F2 analysis of nearly 1000 female mice (12, 15). In fact, we found increased circulating IGF-I concentrations in the congenic 10T as well as parallel changes in hepatic and skeletal IGF-I mRNA expression across several ages. With respect to the skeletal phenotypes of the congenics, 10T female mice at 16 wk had significantly greater BV/TV and trabecular number, compared with B6. This was accompanied by histomorphometric evi-

TABLE 3. Histomorphometry of 10T and B6 at 16 wk of age in the distal femur

Phenotype	B6 males (n = 11)	10T males (n = 11)	B6 females (n = 11)	10T females (n = 11)
BV/*TV* (%)	10.59 ± 0.30	10.80 ± 0.48	6.86 ± 0.58	7.51 ± 0.23[a]
ObS/BS	18.76 ± 1.13	15.05 ± 0.98[a]	22.14 ± 1.36	23.34 ± 2.04
OcS/BS	7.37 ± 0.49	7.41 ± 0.47	10.24 ± 0.44	15.70 ± 1.17[a]
NOc/BP (μm)	3.81 ± 0.30	4.10 ± 0.24	4.93 ± 0.33	6.88 ± 0.66[a]
TbTH (μm)	32.94 ± 1.73	27.44 ± 1.01	25.50 ± 0.64	25.61 ± 0.97
TbSp (μm)	250.0 ± 23.31	223.8 ± 12.28	410.2 ± 27.7	414.32 ± 34.47
TbN (liter/mm)	3.73 ± 0.26	4.07 ± 0.18	2.38 ± 0.13	2.39 ± 0.16

ObS/BS, Osteoblast surface/bone surface; NOc/BP, number of osteoclasts/bone perimeter; TbTH, trabecular thickness; TbSp, trabecular spacing; TbN, trabecular number.
[a] $P < 0.05$ *vs.* B6.

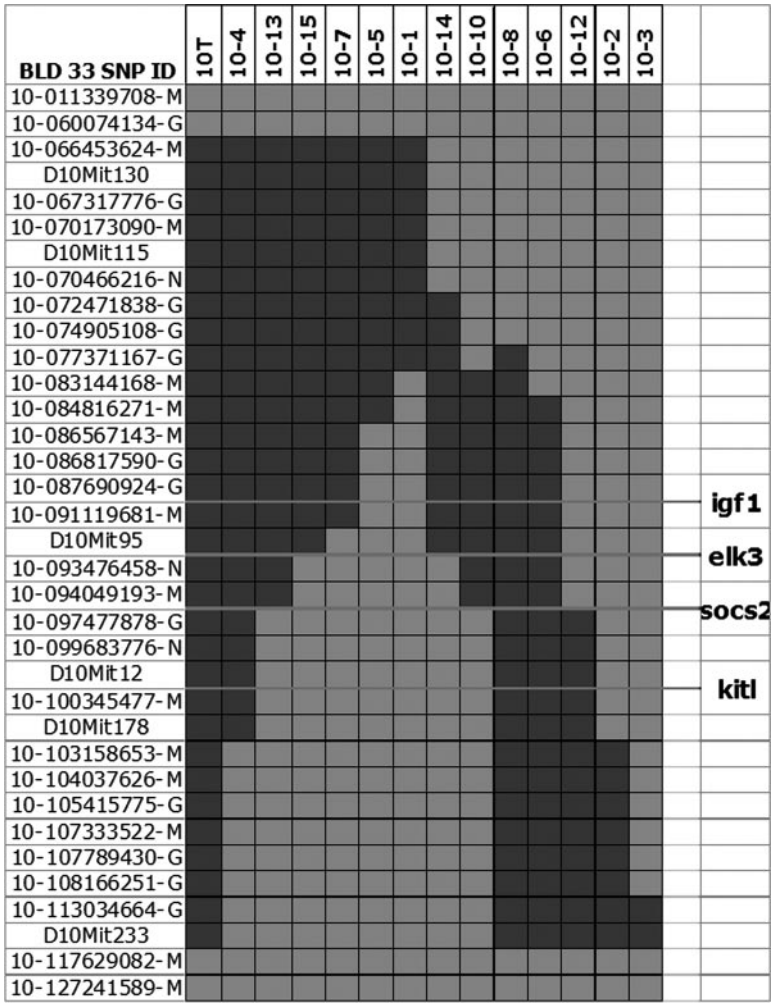

FIG. 2. Nested congenic sublines generated from the 10T congenic. Genetic markers (Mit markers and single-nucleotide polymorphisms) are represented on the y-axis, and on the x-axis, the sublines that were generated to date, and their position on Chr 10 adjacent to their identification. The four major candidate genes are noted in *bold*. *Igf1* is located at 88.7 Mb on this map. Nested sublines 10-15, 10-6, and 10-12 have recently been generated and are being phenotyped.

dence of greater numbers of osteoclasts but not osteoblasts. Taken together, these lines of evidence suggested that 10T mice had a high turnover skeletal phenotype, accompanied by increased serum and skeletal IGF-I. This conclusion is supported by generation of at least one nested congenic subline, 10-4, that recapitulated virtually all of the skeletal phenotypes found in the 10T congenic as well as the increase in serum IGF-I. Moreover, sublines carrying even smaller regions of C3H on a B6 background from recombination within the QTL (10-7, 10-10, 10-13) exhibited even higher serum IGF-I at 16 wk of age than age- and gender-matched B6 controls (*i.e.* a $>$ 20% increase over B6 controls).

Our data provide the first *in vivo* evidence of a functional relationship between allelic differences in IGF-I and bone acquisition. Unlike knockout or transgenic models, congenic mice exhibit only modest differences in circulating and skeletal IGF-I expression. Yet in many ways, the phenotypic feature of these mice parallel changes seen with targeted genomic strategies. For example, we recently showed that targeted overexpression of *Igf1* to bone using a Col1A1 promoter led to greater bone remodeling and increased osteoclastogenesis in adult mice, a finding remarkably similar to the 10T and 10-4 sublines (6). Thus, congenics provide proof of concept that a QTL in the midregion of mouse Chr 10 has a significant effect on both IGF-I expression and bone acquisition.

Because congenics carry allelic differences in a single locus, these mice also reflect the genetic heterogeneity inherent in the human population, thus providing a platform for understanding how heritable differences in IGF-I impact the skeleton (26). For example, the syntenic chromosomal region for mouse Chr 10 in humans is Chr12 q 21–24, which has been reported to have a major femoral BMD QTL in at least three human cohorts (1, 3, 4, 27). And single-nucleotide polymorphisms in the *Igf1* gene have recently been associated with both femoral BMD and circulating IGF-I in a large Chinese sibling cohort (28). Moreover, data from the current study are consistent with recent work identifying a QTL for BV/TV in B6C3F2 progeny in the same region as the *Igf1s2* QTL (15). Two other groups have found BMD QTL in the midregion of Chr 10 in different inbred strain crosses, and Klein *et al.* identified a femoral moment of inertia QTL between B6 and DBA/2 in the same region (29, 30, 31). Hence, there appears to be a conserved locus on mouse Chr 10 in mice and humans that affects both IGF-I and skeletal acquisition.

The phenotypic features of our congenics raise several important and provocative questions. First, there was some degree of gender specificity for the skeletal phenotypes of the

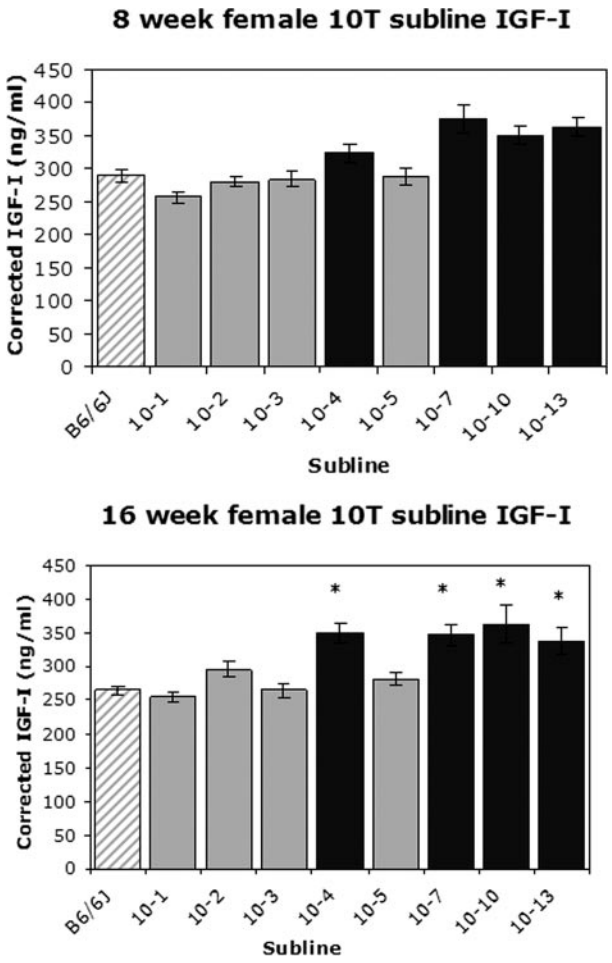

FIG. 3. Differences in serum IGF-I across nested congenic sublines, compared with B6. Serum IGF-I in nanograms per milliliter is the y-axis, congenic sublines on the x-axis. A, At 8 wk, lines 10-4, 10-7, 10-10, and 10-13 are significantly different from B6 controls at $P < 0.05$. B, At 16 wk, the sublines with *asterisks* showed at least a 20% higher serum IGF-I level, compared with B6 (*hatched bars*) ($P < 0.0003$) and had significantly higher IGF-I levels than B6 at 8 wk of age.

sublines. For example, serum IGF-I was increased in both males and female 10T, but differences in BV/TV and osteoclast number, compared with B6, were more pronounced in 10T females than 10T males. A similar pattern was noted in the nested congenic subline 10-4, *i.e.* females exhibited marked increases in trabecular number and connectivity density with increased serum IGF-I, compared with B6, whereas male 10-4 mice showed slightly greater trabecular bone mass but significantly increased serum IGF-I in relation to B6.

TABLE 4. MicroCT and pQCT of 10-4 females and B6 controls at 16 wk of age

	B6	10-4	*P* value
MicroCT	n = 17	n = 14	
Total volume	1.95 ± 0.03	2.07 ± 0.03	0.018[a]
BV/TV	0.078 ± 0.003	0.083 ± 0.003	0.200[b]
Trabecular no.	3.77 ± 0.04	4.14 ± 0.05	<0.0001[b]
Connectivity density	54.56 ± 3.75	76.81 ± 2.89	0.0004[b]
SMI	3.04 ± 0.04	2.89 ± 0.05	0.0315
pQCT	n = 35	n = 24	
Total mineral	10.94 ± 0.125	11.68 ± 0.146	0.0003[a]
Total volume	19.11 ± 0.126	20.03 ± 0.147	<0.001[a]
Midcortical density	1.185 ± 0.004	1.200 ± 0.005	0.030[a]

[a] Body weight was a significant covariate.
[b] Femur length was a significant covariate.

Gender specificity for skeletal phenotypes has been described previously (24). Both Klein *et al.* and our group (17, 31) have reported gender differences for peak bone mass and serum IGF-I among congenic strains. The mechanisms surrounding this feature of QTL analysis are not clear yet are probably more frequent than reported. It should be noted that we mapped QTL for BMD and IGF-I in the original B6C3F2 progeny by phenotyping female mice only (12). Hence, we do not know whether male F2 mice would have a QTL for serum IGF-I and BMD in the same mid region of Chr 10. But QTL studies in progress, particularly in *lit/lit* mice on a C3H and B6 background, may help define gender specificity and its relationship to the GH/IGF-I axis (32).

We still to need clarify the relationship between genes controlling circulating IGF-I and those influencing bone acquisition. The Chr 10 QTL region represents approximately 57 Mb of genomic DNA with hundreds of genes that could influence both IGF-I and bone mass. Conversely, the QTL may possess two sets of genes for these phenotypes: one that regulates IGF-I expression and one that independently contributes to bone acquisition. Only through extensive skeletal phenotyping of the congenic sublines (*e.g.* 10-7 or 10-10), which carry a much narrower genomic region than 10-4, will we be able to determine how many genes may be present in this region and which ones regulate circulating and/or skeletal IGF regulatory pathways. Those studies are currently ongoing.

Another surprising finding was the developmental differences in serum IGF-I in the nested congenic sublines, compared with B6 progenitors. Several years ago we noted that in B6 females, between 8 and 16 wk, there was a modest but statistically significant decline in circulating IGF-I, not seen in female C3H mice (11). As we developed congenic sublines including 10T, we noted that differences in serum IGF-I in these strains were considerably greater at 16 than 8 wk of age, compared with age-matched B6 controls (*i.e.* > 20%). This was due to a decline in serum IGF-I for B6 during the late phases of pubertal growth, whereas serum IGF-I in the sublines either did not change or increased. Similarly, the bone phenotype in the congenics was much more pronounced at 16 *vs.* 8 wk of age. These developmental differences resemble changes in female C3H mice during this period and strongly suggest that the genomic region of interest in mouse Chr 10 is temporally regulated. Whether this is due to enhanced growth hormone sensitivity, changes in sex steroids, or other factors remains to be determined.

With respect to identifying where the alleles are positioned that result in the IGF-I and skeletal phenotypes of the congenics, there are several plausible candidate genes. The 10T, 10-4, 10-7, 10-10, and 10-13 congenic mice all carry *Igf1* alleles from C3H, making it conceivable that a *cis*-acting polymorphism within that gene, or an enhancer adjacent to the *Igf1* gene, could affect transcriptional activity. We previously found a polymorphic sequence in the P1 promoter B6 in the *Igf1* gene that differed between C3H and that may be re-

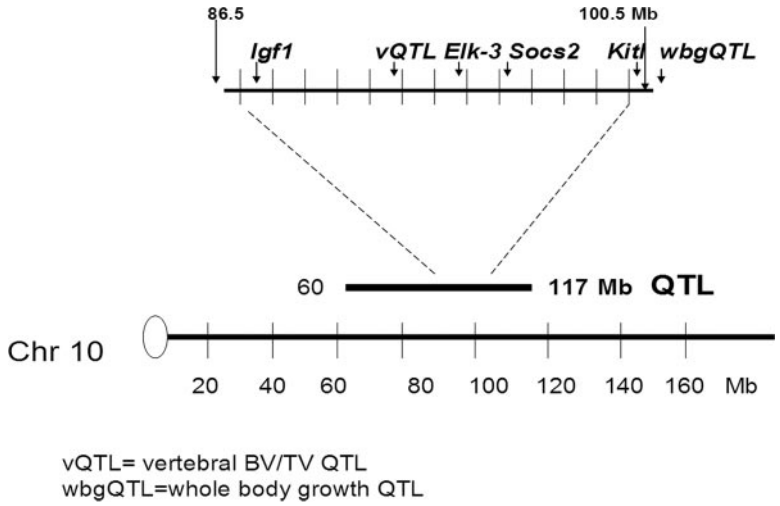

FIG. 4. Candidate genes in the narrowed QTL region including two important and possibly overlapping QTL mapped by other investigators [vertebral BV/TV QTL (vQTL) and whole-body growth QTL (wbgQTL)]. Mb, Megabases. Based on Fig. 2, our region encompasses approximately 18.3 Mb of genomic DNA; approximately 148 genes are found in this region.

sponsible for increased transcription (14). We recently also identified a single nucleotide polymorphism in the 3′-untranslated region of the *Igf1* gene between B6 and C3H that might affect message stability and is currently being investigated. Interestingly, two other groups (33, 34) have also found QTL in the same Chr 10 region for *Igfbp-5* and *Igfbp-3*, two IGFBPs that are regulated by IGF-I. Moreover, association studies in humans have reported polymorphisms in the IGF-I gene and serum levels of the protein (1).

Another candidate gene in this QTL is *Socs-2,* suppressor of cytokine signaling. It inhibits GH-mediated induction of IGF-I and knockout of this gene results in gigantism with increased body weight and greater femoral length (35). However, several lines of evidence suggest that *Socs-2* is not a candidate gene. First, before narrowing the sublines, we measured hepatic *Socs-2* expression by RPA in 10T and found slightly higher levels in 10T *vs.* B6 (Adamo, M. L., personal communication). This would not be consistent with either the skeletal or IGF-I phenotype of 10T or 10-4. Second, the 10-7 subline does not carry the *Socs*-2 gene yet has higher serum IGF-I than B6. Thus, we suspect *Socs-2* is not the gene driving the skeletal or IGF-I phenotypes in the 10 sublines. But the proximity of this gene to *Igf1* demonstrates how structural aspects of the mammalian genome align nicely with functional components.

We can eliminate another candidate, *Kitl*, a protein that can stimulate osteoclast recruitment because it is outside the locus identified from our new sublines (see Fig. 2). On the other hand, *Elk-3*, a transcription factor, is located closer to the *Igf1* gene and currently cannot be excluded. There is one report (36) of a targeted mutation in *Elk-3* that is associated with early lethality due to vascular defects and chylothorax. Although this gene is an unlikely candidate, it is conceivable that the *Igf1s2* QTL could carry a gene such as *Elk-3*, which targets expression of early genes in development, and thereby affects peak bone mass by up-regulating IGF-I transcription (36). Indeed, our group recently reported a strong QTL for areal BMD in the same region on Chr 10(*i.e.* ~60 cM) in F2 female mice from a B6 × 129 cross (29). This would imply conservation across inbred strains of a gene or genes that affect peak bone acquisition.

Finally, with respect to the skeletal phenotype, several lines of evidence suggest there may be increased osteoclastic activity in the 10T and 10-4 congenic female mice. We found that 16-wk 10T females had higher BV/TV than B6; this was associated with greater numbers of osteoclasts and more trabeculae. The 10-4 subline also had more trabeculae, greater bone volume, lower SMI, and increased trabecular connectivity, compared with B6. These findings would be consistent with a high bone turnover state, particularly by 16 wk of age, a time when there are major differences in circulating IGF-I, compared with the progenitors. Whether these findings are related to increased skeletal IGF-I expression in all the major sublines is not clear yet. Nevertheless, IGF-I can stimulate bone remodeling and particularly bone resorption when administered exogenously to mice and rats or when overexpressed in bone (37). The mechanism for IGF-I induction of osteoclastogenesis is not well delineated, but IGF-I can stimulate receptor activator of nuclear factor-κB ligand expression in ST-2 cells (25). Further studies will more clearly define the skeletal phenotype in the nested congenic sublines and the role of IGF-I in bone remodeling.

In summary, we generated nested congenic mice that have increased circulating IGF-I and a pronounced skeletal phenotype. These sublines are important model systems not only for dissecting the relationship between allelic differences in local/systemic IGF-I and bone acquisition but also for identifying heritable determinants of IGF-I expression.

Acknowledgments

Received March 3, 2006. Accepted April 24, 2006.

Address all correspondence and requests for reprints to: Clifford J. Rosen, M.D., The Jackson Laboratory, 600 Main Street, Bar Harbor, Maine 04609. E-mail: rofe@aol.com.

This work was supported by National Institute of Arthritis and Musculoskeletal and Skin Diseases AR45433 and AR 38933.

Disclosure: K.M.D., K.L.S., G.A.G., B.K.-J., M.L.A., L.R.D., C.A.-B., W.G.B., C.J.R., and L.G.H. have nothing to declare. J.L. has received consulting fees of less than $10,000 and has equity ownership/stock options of less than $10,000; and B.E.K. has disclosed receipt of lecture fees of less than $10,000.

References

1. **Niu T, Rosen CJ** 2005 The insulin-like growth factor-I gene and osteoporosis: a critical appraisal. Gene 361:38–56

2. **Beamer WG, Shultz KL, Donahue LR, Churchill GA, Sen S, Wergedal JR, Baylink DJ, Rosen CJ** 2001 Quantitative trait loci for femoral and lumbar vertebral bone mineral density in C57BL/6J and C3H/HeJ inbred strains of mice. J Bone Miner Res 16:1195–1206
3. **Deng HW, Xu FH, Huang QY, Shen H, Deng H, Conway T, Liu YJ, Liu YZ, Li JL, Zhang HT, Davies KM, Recker RR** 2002 A whole-genome linkage scan suggests several genomic regions potentially containing quantitative trait loci for osteoporosis. J Clin Endocrinol Metab 87:5151–5159
4. **Karasik D, Myers RH, Cupples LA, Hannan MT, Gagnon DR, Herbert A, Kiel DP** 2002 Genome screen for quantitative trait loci contributing to normal variation in bone mineral density: the Framingham Study. J Bone Miner Res 17:1718–1727
5. **Lupu F, Terwilliger JD, Lee K, Segre GV, Efstratiadis A** 2001 Roles of growth hormone and insulin-like growth factor 1 in mouse postnatal growth. Dev Biol 1:141–162
6. **Jiang J, Lichtler AC, Gronowicz GG, Adams DJ, Rosen CJ, Kream BE** 28 April 2006 Transgenic mice with osteoblast targeted IGF-I show increased growth and remodeling. Bone 10.1016/j.bone.2006.02.068
7. **Zhang M, Xuan S, Bouxsein ML, von Stechow D, Akeno N, Faugere MC, Malluche H, Zhao G, Rosen CJ, Efstratiadis A, Clemens TL** 2002 Osteoblast-specific knockout of the insulin-like growth factor (IGF) receptor gene reveals an essential role of IGF signaling in bone matrix mineralization. J Biol Chem 277:44005–44012
8. **Mochizuki H, Hakeda Y, Wakatsuki N, Usui N, Akashi S, Sato T, Tanaka K, Kumegawa M** 1992 Insulin-like growth factor-I supports formation and activation of osteoclasts. Endocrinology 131:1075–1080
9. **Rivadeneira F, Houwing-Duistermaat JJ, Beck TJ, Janssen JA, Hofman A, Pols HA, Van Duijn CM, Uitterlinden AG** 2004 The Influence of an insulin-like growth factor i gene promoter polymorphism on hip bone geometry and the risk of nonvertebral fracture in the elderly: the Rotterdam Study. J Bone Miner Res 19:1280–1290
10. **Rosen CJ, Kurland ES, Vereault D, Adler RA, Rackoff PJ, Craig WY, Witte S, Rogers J, Bilezikian JP** 1998 Association between serum insulin growth factor-I (IGF-I) and a simple sequence repeat in IGF-I gene: implications for genetic studies of bone mineral density. J Clin Endocrinol Metab 83:2286–2290
11. **Rosen CJ, Dimai HP, Vereault D, Donahue LR, Beamer WG, Farley J, Linkhart S, Linkhart T, Mohan S, Baylink DJ** 1997 Circulating and skeletal insulin-like growth factor-I (IGF-I) concentrations in two inbred strains of mice with different bone mineral densities. Bone 21:217–223
12. **Rosen CJ, Churchill GA, Donahue LR, Shultz KL, Burgess JK, Powell DR, Ackert C, Beamer WG** 2000 Mapping quantitative trait loci for serum insulin-like growth factor-1 levels in mice. Bone 27:521–528
13. **Adamo ML, Ma X, Ackert Bicknell CL, Donahue LR, Beamer WG, Rosen CJ** 2006 Genetic increase in serum insulin-like growth factor-I (IGF-I) in C3H/HeJ compared to C57BL/6J mice is associated with increased transcription from the IGF-I exon 2 promoter. Endocrinology PM:16527837
14. **Iida K, Rosen CJ, Ackert-Bicknell CL, Thorner MO** 2005 Genetic differences in the IGF-I gene among inbred strains of mice with different serum IGF-I levels. J Endocrinol 186:481–489
15. **Bouxsein ML, Uchiyama T, Rosen CJ, Shultz KL, Donahue LR, Turner CH, Sen S, Churchill GA, Muller R, Beamer WG** 2004 Mapping quantitative trait loci for vertebral trabecular bone volume fraction and microarchitecture in mice. J Bone Miner Res 19:587–599
16. **Bouxsein ML, Rosen CJ, Turner CH, Ackert CL, Shultz KL, Donahue LR, Churchill G, Adamo ML, Powell DR, Turner RT, Muller R, Beamer WG** 2002 Generation of a new congenic mouse strain to test the relationships among serum insulin-like growth factor I, bone mineral density, and skeletal morphology *in vivo*. J Bone Miner Res 17:570–579
17. **Rosen CJ, Ackert-Bicknell CL, Adamo ML, Shultz KL, Rubin J, Donahue LR, Horton LG, Delahunty KM, Beamer WG, Sipos J, Clemmons D, Nelson T, Bouxsein ML, Horowitz M** 2004 Congenic mice with low serum IGF-I have increased body fat, reduced bone mineral density, and an altered osteoblast differentiation program. Bone 35:1046–1058
18. **Rosen CJ, Ackert-Bicknell C, Beamer WG, Nelson T, Adamo M, Cohen P, Bouxsein ML, Horowitz MC** 2005 Allelic differences in a quantitative trait locus affecting insulin-like growth factor-I impact skeletal acquisition and body composition. Pediatr Nephrol 20:255–260
19. **Shultz KL, Donahue LR, Bouxsein ML, Baylink DJ, Rosen CJ, Beamer WG** 2003 Congenic strains of mice for verification and genetic decomposition of quantitative trait loci for femoral bone mineral density. J Bone Miner Res 18:175–185
20. **Akilesh S, Shaffer DJ, Roopenian D** 2003 Customized molecular phenotyping by quantitative gene expression and pattern recognition analysis. Genome Res 13:1719–1727
21. **Dheda K, Huggett JF, Bustin SA, Johnson MA, Rook G, Zumla A** 2004 Validation of housekeeping genes for normalizing RNA expression in real-time PCR. Biotechniques 37:112–114
22. **Masson P** 1929 Trichrome stainings and their preliminary technique. J Tech Meth 12:75–90
23. **Parfitt AM, Drezner MK, Glorieux FH, Kanis JA, Malluche H, Meunier PJ, Ott SM, Recker RR** 1987 Bone histomorphometry: standardization of nomenclature, symbols, and units. Report of the ASBMR Histomorphometry Nomenclature Committee. J Bone Miner Res 2:595–610
24. **Vaughn TT, Pletscher LS, Peripato A, King-Ellison K, Adams E, Erikson C, Cheverud JM** 1999 Mapping quantitative trait loci for murine growth: a closer look at genetic architecture. Genet Res 74:313–322
25. **Rubin J, Ackert-Bicknell CL, Zhu L, Fan X, Murphy TC, Nanes MS, Marcus R, Holloway L, Beamer WG, Rosen CJ** 2002 IGF-I regulates osteoprotegerin (OPG) and receptor activator of nuclear factor-κB ligand *in vitro* and OPG *in vivo*. J Clin Endocrinol Metab 87:4273–4279
26. **Fehr C, Shirley RL, Belknap JK, Crabbe JC, Buck KJ** 2002 Congenic mapping of alcohol and pentobarbital withdrawal liability loci to a <1 centimorgan interval of murine chromosome 4: identification of Mpdz as a candidate gene. J Neurosci 22:3730–3738
27. **Mitchell BD, Bauer RI, Perez R** 1998 Genome-wide scan for loci influencing bone density in Mexican Americans. Am J Hum Genet 63:301
28. **Hsu Y, Delahunty KM, Niu T, Terwedow H, Lorenzo JA, Kream BE, Xu X, Rosen CJ** 2005 Moving between mouse and humans to identify a candidate gene on Chr 10 that affects serum IGF-I, bone turnover and bone mineral density. J Bone Miner Res 20:S54
29. **Ishimori N, Li R, Walsh KA, Korstanje R, Rollins JA, Petkov P, Pletcher MT, Wiltshire T, Donahue LR, Rosen CJ, Beamer WG, Churchill GA, Paigen B** 2006 Quantitative trait loci that determine BMD in C57BL/6J and 129S1/SvImJ inbred mice. J Bone Miner Res 21:105–112
30. **Drake TA, Schadt E, Hannani K, Kabo JM, Krass K, Colinayo V, Greaser 3rd LE, Goldin J, Lusis AJ** 2001 Genetic loci determining bone density in mice with diet-induced atherosclerosis. Physiol Genomics 5:205–215
31. **Klein RF, Allard J, Avnur Z, Nikolcheva T, Rotstein D, Carlos AS, Shea M, Waters RV, Belknap JK, Peltz G, Orwoll ES** 2004 Regulation of bone mass in mice by the lipoxygenase gene Alox15. Science 303:229–232
32. **Donahue LR, Beamer WG, Schultz K, Hurd J, Guido V, Rosen CJ** 2005 QTL for bone and body composition phenotypes are sex specific in a mouse model GH/IGF-I deficiency. J Bone Miner Res 20:S232
33. **Mohan S, Masinde G, Li X, Baylink DJ** 2003 Mapping quantitative trait loci that influence serum insulin-like growth factor binding protein-5 levels in F2 mice (MRL/MpJ X SJL/J). Endocrinology 144:3491–3496
34. **Brockmann GA, Haley CS, Wolf E, Karle S, Kratzsch J, Renne U, Schwerin M, Hoeflich A** 2001 Genome-wide search for loci controlling serum IGF binding protein levels of mice. FASEB J 15:978–987
35. **Metcalf D, Greenhalgh CJ, Viney E, Willson TA, Starr R, Nicola NA, Hilton DJ, Alexander WS** 2000 Gigantism in mice lacking suppressor of cytokine signalling-2. Nature 405:1069–1073
36. **Ayadi A, Zheng H, Sobieszczuk P, Buchwalter G, Moerman P, Alitalo K, Wasylyk B** 2001 Net-targeted mutant mice develop a vascular phenotype and up-regulate egr-1. EMBO J 20:5139–5152
37. **Rosen HN, Chen V, Cittadini A, Greenspan SL, Douglas PS, Moses AC, Beamer WG** 1995 Treatment with growth hormone and IGF-I in growing rats increases bone mineral content but not bone mineral density. J Bone Miner Res 10:1352–1358

***Endocrinology* is published monthly by The Endocrine Society (http://www.endo-society.org), the foremost professional society serving the endocrine community.**